Technical Note on EtfAG Entry for MLDC Round 3.3

Jonathan R Gair*
Institute of Astronomy, Madingley Road, CB3 0HA, Cambridge, UK

Ilya Mandel†
Department of Physics and Astronomy, Northwestern University, 2131 Tech Dr., Evanston, IL 60208
(Dated: May 1, 2009)

We carried out an analysis of Mock LISA Data Challenge 3.3 using time-frequency techniques. As in challenges 1B.3.*, we used a Chirp-based Algorithm for Track Search (CATS) to locate tracks characterized by frequency and its first two derivatives on a spectrogram of the data [1, 2]. We have made significant improvements to the CATS algorithm for this challenge, which we briefly describe below. However, due to low signal SNR and multiple overlapping signals, we were only able to convincingly estimate one set of tracks corresponding to a single source of type 2–3. We made rough estimates of the intrinsic parameters of this source based on the track shape only and of the sky position using the power variation along the track [3, 4].

I. TRACK DETECTION: CATS

We used an improved version of the Chirp-based Algorithm for Track Search [1, 2] to find tracks on a time-frequency spectrogram. CATS is essentially a grid-based search on a spectrogram for tracks of a given shape. For the EMRI challenge 3.3, we parametrized chirping tracks by three parameters: frequency f and its first two time derivatives $\dot{f}$ and $\ddot{f}$. (The third time derivatives of frequency along the tracks are vanishingly small for low-eccentricity signals like those of type 1 and type 2–3; it can be neglected for tracks of type 4–5 if sufficiently short sections of the tracks are fitted.) Moreover, the first and second time derivative of frequency must be positive.

A CATS search proceeds as follows:

- Construct A and E channels from the bandpassed challenge data stream (we used Synthetic LISA data).
- For each channel, construct a spectrogram by dividing the data into overlapping time segments of equal duration, then Fourier transforming the data in each time segment after multiplying it by a Hanning window to reduce edge effects.
- Normalize the two spectrograms by dividing the signal power in each pixel by the expected LISA noise power spectral density, then construct a joint spectrogram by adding the two normalized spectrograms.
- Construct a grid of parameters in the $(f, \dot{f}, \ddot{f})$ space.
- For each point in the parameter space, build a potential track and determine the power in the pixels along this track.
- Compute the CATS track power statistic which is chosen to optimize track detection for a given false alarm probability. For this search, the CATS power statistic was equal to

$$\frac{P - 4N}{\sqrt{N}},$$

  where P is the sum of the power in all pixels along a track and N is the number of pixels that a track passes through; in the absence of a signal we expect the power in a pixel of pure noise to be a χ^2 variable of degree 4. Keep a list of all tracks that exceed a power statistic chosen to yield only tracks exceeding a fixed false alarm probability.
- Sort all found tracks by the CATS power statistic.

*Electronic address: `jgair@ast.cam.ac.uk`
†Electronic address: `ilyamandel@chgk.info`

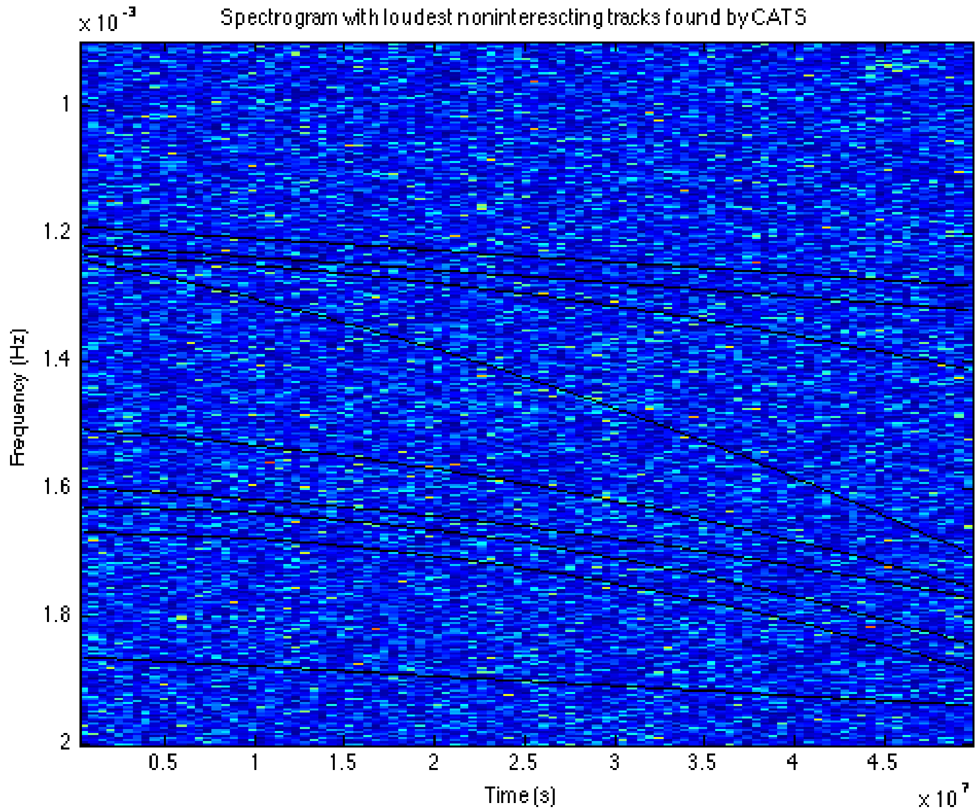

FIG. 1: A spectrogram of a portion of the data from C3.3 with the tracks detected by CATS plotted over in black.

- Go down the list of sorted tracks and retain only those tracks which do not share any pixels with the tracks above them; thus, construct a sorted list of non-overlapping tracks whose power statistic exceeds a threshold.

Figure [**?**] shows a spectrogram of a portion of the Challenge 3.3 data, overplotted with tracks detected by CATS.

A number of parameters in the above procedure can be varied. These include the starting and ending time of the search, the lower and upper frequencies of the search window, and the duration of time bins used to create the spectrogram (typically, wider bins are desirable to search for weaker, slowly evolving signals).

Additionally, searches can be constrained to a more narrow region of the parameter space. For example, such a constraint can be useful when searching for weaker sidebands of an already detected track caused by orbital-plane precession. We can restrict the search to tracks that are nearly parallel to the detected track (same $\dot{f}$) and offset by a small frequency separation, thereby reducing the volume of the parameter space to be searched, allowing us to lower the detection threshold.

Varying these parameters can produce different sets of tracks. Figure **??** shows a sample of such tracks (different colors correspond to sets of tracks detected by CATS searches with different search parameters, as described above). The CATS power statistic is used to determine when we have achieved the most confident fit. However, in the presence of noise, and with possible overlapping signals, it was not always possible to determine the track parameters precisely. For example, the following table shows the possible spread in the parameters of a strong track found on a spectrogram with time bins of duration 65536×15s lasting from $T = 0$ to $T = 3e7$s, the region where this tracks is strongest. The small differences in the power statistic indicate that while f_0 can be measured to an accuracy of a few $\times 10^{-7}$Hz, the accuracy in $\ddot{f}_0$ is only $\sim 10^{-21}$ Hz s^{-2} (the subscript 0 specifies that all quantities are defined at $T = 0$).

CATS power stat.	f_0 (Hz)	fdot_0 (Hz/s)	fddot_0 (Hz/s/s)
41.83061365	0.001219431559	1.669036865e-12	1.971675984e-20
41.77076008	0.001219024658	1.755826782e-12	1.445895722e-20

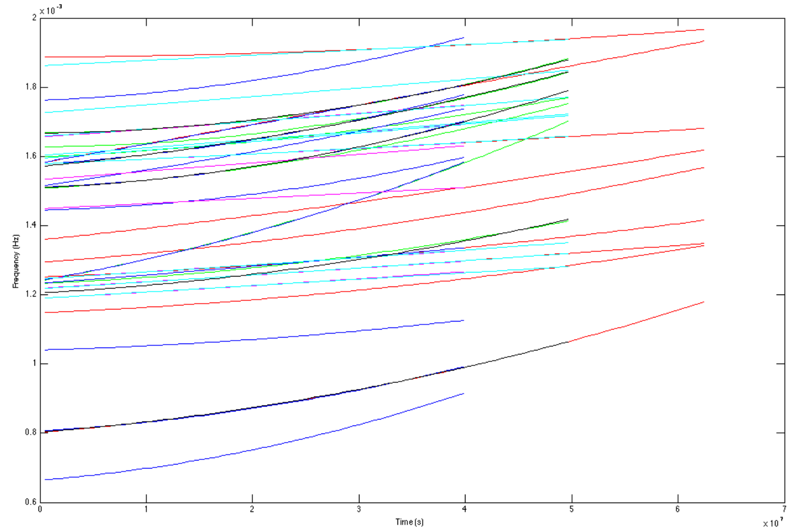

FIG. 2: A sample of tracks detected by CATS for Challenge 3.3. Different colors correspond to sets of tracks detected by CATS searches with different search parameters, as described in the text.

41.76940698	0.001219431559	1.675713013e-12	1.884045941e-20
41.7613895	0.001219431559	1.669036865e-12	1.884045941e-20
41.7613895	0.001219482421	1.662360718e-12	1.927860962e-20
41.75194303	0.001218516031	1.842616699e-12	7.448553719e-21

II. TRACK SEARCH RESULTS

We clearly identified a sequence of tracks ($n = 2$ and $n = 3$ harmonics and sidebands) corresponding to a source of type 2–3. The parameters of these tracks, with their presumed identification, are listed below.

Brightest track, presumably $n = 2$ harmonic, $m = -1$ sideband:

$$[f_0, \dot{f}_0, \ddot{f}_0] = [\texttt{0.001217651366} \quad \texttt{1.927573948e-12} \quad \texttt{4.856543947e-21}]$$

The $m = 0$ sideband:

$$[f_0, \dot{f}_0, \ddot{f}_0] = [\texttt{0.001246134439} \quad \texttt{1.9478642e-12} \quad \texttt{6.475391929e-21}]$$

(Note, however, that attempts to estimate f_0 alone based on shorter track segments yielded values of $f_0 = 0.00121948$Hz and $f_0 = 0.00125397$Hz, respectively, for these two tracks).

The $m = -2$ sideband:

$$[f_0, \dot{f}_0, \ddot{f}_0] = [\texttt{0.001189931299} \quad \texttt{1.741497661e-12} \quad \texttt{8.766914965e-21}]$$

The brightest track, $n = 3$ harmonic:

$$[f_0, \dot{f}_0, \ddot{f}_0] = [\texttt{0.001594034934} \quad \texttt{2.347235978e-12} \quad \texttt{7.514498541e-21}]$$

Its possible sidebands:

$$[f_0, \dot{f}_0, \ddot{f}_0] = [\texttt{0.001656087348} \quad \texttt{2.145323206e-12} \quad \texttt{7.514498541e-21}]$$

$$[f_0, \dot{f}_0, \ddot{f}_0] = [\texttt{0.001725260413} \quad \texttt{2.313088738e-12} \quad \texttt{6.475391929e-21}]$$

$$[f_0, \dot{f}_0, \ddot{f}_0] = [\texttt{0.001532491145} \quad \texttt{2.448192364e-12} \quad \texttt{0}]$$

We could not get an accurate plunge-time measurement; based on the fact that no tracks could be found in the relevant parameter range for times above $5e7$s, we assumed this value for the plunge time.

We found some tracks suggesting the existence of a second source of type 2–3. However, we could not separate it well from source described above, and did not attempt to estimate its parameters.

We were not able to find a convincing track of type 1 (we had a candidate for the $n = 3$ harmonic, but could not identify the $n = 2$ harmonic).

We did not search carefully for tracks of type 4–5. Such tracks would be rapidly searching, making it difficult to fit the entire track with a single set of parameters. Also, the computational load on CATS scales as the cube of the number of frequency bins in the region of the spectrogram being considered, making such searches computationally expensive. However, a cursory search did not reveal strong track candidates.

III. PARAMETER ESTIMATION

We estimated 8 parameters for the well-identified source described above: the two masses, eccentricity and frequency at $t = 0$, SMBH spin, spin-orbital angle λ, and two sky direction angles. If at any time during the observation two harmonics of the orbital frequency are detected, plus a sideband of one of those harmonics arising due to the orbital plane precession, then we can measure the three fundamental frequencies at that time. The orbital frequency, ν, is an intrinsic parameter and, for a choice of eccentricity, e, and orbital inclination, λ, the orbital plane precession frequency, f_α, determines the black hole spin, S, while the perihelion precession frequency, f_γ, determines the central black hole mass, M. If the derivative of a harmonic is also measured, then the compact object mass, m, can also be determined for specified e and λ. If we have an estimate of the plunge time, t_p, and an estimate of at least one of the frequency components at another time, it is possible to iterate over e and λ to obtain a crude estimate of the intrinsic parameters [1]. We thus employed the first step of the technique described in [1] to measure the following parameter values:

```
EclipticLatitude (Radian): 1.00
EclipticLongitude (Radian): 1.46
MassOfSMBH (SolarMass): 4812175.542
MassOfCompactObject (SolarMass): 9.748272428
Spin (MassSquared): 0.6479682688
InitialAzimuthalOrbitalFrequency (Hertz): 0.0003748197021
InitialEccentricity (Unit): 0.1901889567
LambdaAngle (Radian): 0
Probability (relative): 1
```

We did not estimate PolarAngleOfSpin, AzimuthalAngleOfSpin, the initial phase angles, or the distance to the source.

[1] Gair JR, Mandel I and Wen L, CQG 25, 184031; arXiv:0804.1084
[2] Mandel I and Gair J R, in preparation
[3] Gair J R, Mandel I and Wen L, 2007, arXiv:0710.5250
[4] Wen L, Chen Y and Gair J R, 2006, Laser Interferometer Space Antenna: 6th International LISA Symposium, 873, 595